International Journal of Applied Engineering Research ISSN 0973-4562 Volume 13, Number 15 (2018) pp. 11781-11792

Effect of Varying Throat Location in Wind Load Response of Natural Draught Hyperboloid Cooling Tower

Prof. S .Vijaya Bhaskar Reddy
Head Of The Department of civil Engineering, CMR Technical Campus, Kandlakoya(V),Medchal(M),R.R Dist.,Telangana, India.

Borla.Rajagopal
Student, In Structural Engineering, CMR Technical Campus, Kandlakoya(V),Medchal(M),R.R Dist.,Telangana, India.

Abstract

Thermal and Nuclear power stations require a large amount of cooling water to condense the boiler steam. Because of this, cooling water gets heated and to cool this for further use, the excess heat is removed inside cooling towers. In Natural Draft Cooling Towers (NDCTs) the difference in density of warm air inside and the colder air outside creates the natural draft in the interior. Evaporative cooling occurs as the warm water meets the rising cooler air.

These structures contribute to power generation efficiency and environmental protection. Hyperbolic shape is preferred due to its large base area, strength and stability. The towers involve considerable amount of work on structural design aspect. The predominant forces acting on the cooling tower will result from wind loading. The reinforcement design of NDCT is controlled mainly by the net difference between the tension due to wind loading and compression due to dead load. Also, the design is sensitive to the vertical and circumferential variation of wind pressure around the tower.

This paper deals with the study of eight typical NDCT models, all with Base diameter of 104m, Top diameter of 62m, height 135m above ground level and throat location varying from 70% to 87.5% of total height. The wind loads have been calculated using the circumferentially distributed design wind pressure coefficients along with the design wind pressures at different levels. Meridional and circumferential distributions of membrane forces due to wind load for varying throat location has been studied and observations are discussed. It is observed that throat location plays a vital part in economic design of the structure.

Keywords: These structures are most efficient measures for cooling in thermal power plants by minimizing the need of water & avoiding thermal pollution of water bodies. Natural Draft Cooling Towers presently form the largest reinforced concrete shell structures in the world.

INTRODUCTION

Thermal power is the "largest" source of power in India. There are different types of thermal power plants based on the fuel used to generate steam such as coal, gas, and Diesel. About 71% of electricity consumed in India are generated by thermal power plants. In a thermal power station, heated steam drives the turbo generator which produces electric energy. To create an efficient heat sink at the end of this process, the steam is condensed and recycled into the boiler. This requires a large amount of cooling water, whose temperature is raised and then re cooled in structures called cooling tower.

Cooling towers make use of evaporation whereby some of the water is evaporated into a moving air stream and subsequently discharged into the atmosphere. As a result, the remainder of the water is cooled down significantly.

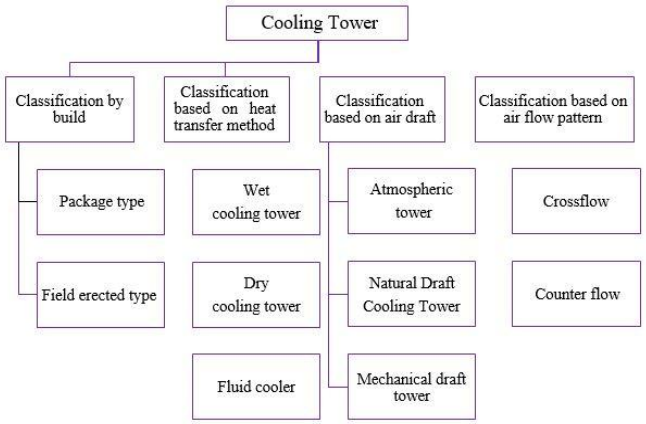

Figure 1: Types of cooling towers

Natural draft hyperbolic cooling tower makes use of the temperature difference between the ambient air and the hotter air inside the tower. In this tower, the heated water is distributed evenly through channels and pipes above the fill. As hot air moves upwards through the tower due to lower density, fresh cool air is drawn into the tower through bottom air inlets. As the water flows and drops through the fill sheets, it comes into contact with the rising cooler air. Evaporative cooling occurs, and the cooled water is then collected in the water basin to be recycled into the condenser. A natural draft tower is so called because natural flow of air occurs through tower without the use of fan.

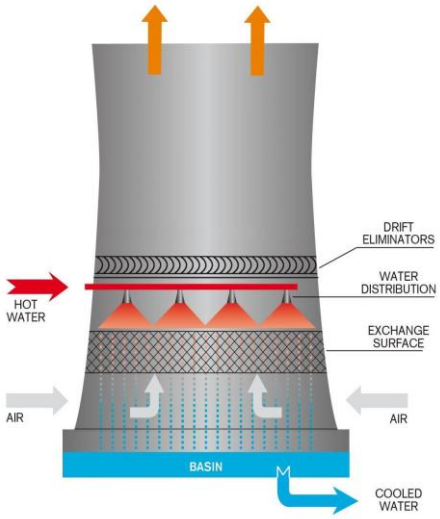

Figure 1.2. Working of natural draft cooling tower

A typical NDCT consists of a shell body, supporting columns, fill support, cold water basin and water distribution system. The principal function of the hyperbolic shell is to create a draft of air. The cooling tower shell is supported by a truss or framework of columns bridging the air inlet to the tower foundation. The entire structure is made of high-strength Reinforced Cement Concrete (RCC) in the form of hyperbolic thin shell standing on diagonal, meridional, or vertical supporting columns and radial supports.

The geometry of NDCT is made of doubly curved hyperboloid surface. Hyperboloid is a solid surface having plane sections that are hyperbolas. The hyperbolic form of thin-walled towers provides optimum conditions for good aerodynamics, strength, and stability.

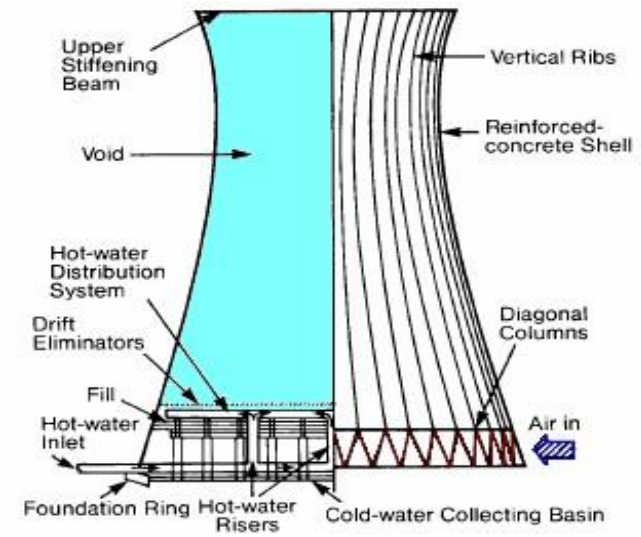

Figure 1.3. Natural draft cooling tower.

The only general ruled surface of revolution which can degenerate into a cylinder, a cone, or a plane is the hyperboloid. A hyperboloid of revolution of one sheet can be obtained by revolving a hyperbola around its semi minor axis. Hyperboloid is a doubly ruled surface; thus, it can be built with straight lines, producing a strong structure at a lower cost than other methods. Hyperboloid's geometry offers high structural stability as well as structural economy. The hyperbolic geometry has advantage of a negative Gaussian curvature which makes it superior in stability against external pressures than straight towers

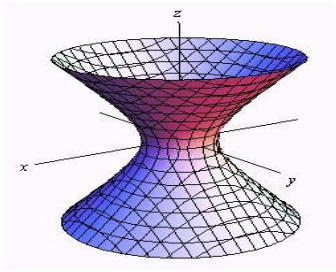

Figure 1.4. Hyperboloid

The widened bottom of the tower accommodates large installation of fill to facilitate the evaporative cooling of the thin film of circulated water. Narrowing effect of the tower accelerates the laminar flow of evaporation and diverging top promotes turbulent mixing which increases the contact between hot inside air and cooler outside air. Hyperboloid shape is mainly recommended for NDCTs due to following reasons:

- Air gets smoothly directed towards center due to the strong upward draft created by the shape.
- Increased base area which allows more fill packing.
- Greater structural strength and stability provided by this shape.
- Hyperboloid offers very substantial material economies compared with other shapes.
- From the structural point of view NDCT are high rise reinforced concrete structures in the form of doubly curved thin walled shells of complex geometry and so is their analysis and design. The in-plane membrane actions primarily resist the applied forces and bending plays the secondary role in these special structures.

Problem statement

Their very small shell thickness, sheer size and sensitiveness to horizontal loads make these towers exceptional structures. Today's natural draft cooling towers are safe and durable structures if properly designed and constructed. Nevertheless, it should be recognized that this high-quality level has been achieved only after the lessons learned from a series of collapsed or heavily damaged towers have been incorporated into the relevant body of engineering knowledge.

Objectives

The elements of the cooling tower should be reinforced with deformed steel bars to provide for the tensile forces and moments arising from the controlling combination of factored loading cases. The reinforcement design is based on the distribution of meridional and circumferential stresses.

The objective of this project is:

- To study the distribution of meridional stresses due to Self-weight, wind load, and their combination
- To study the distribution of Circumferential/Hoop stresses due to Self- weight, wind load, and their combination
- To analyze the effect of varying throat location in membrane stress distribution, both meridional and circumferential stresses, of the cooling tower.

The project will focus on analysing a typical NDCT under static loads due to self- weight and dynamic loads arising out of wind. Analysis will be carried out using finite element based software STAAD Pro.

Modeling

Typical geometry made of a top and bottom hyperbola (above and below throat) is taken. Eight models with throat at different locations are modeled for study. Total height, top diameter, bottom diameter, throat diameter is common for all eight models. Height of throat from bottom (H_b) is different for all the eight models.

Table 1.1: Model dimensions variation (Common for all 10 models)

1	Total height	135m
2	Column height	10m
3	Total shell height(H)	125m
4	Top diameter ($2 \times r_t$)	62m
5	Bottom diameter ($2 \times r_b$)	104m
6	Throat diameter ($2 \times r_t$)	60m

Table 1.2: Throat location

Model	Throat location	H_b(m)
1	70.00%	87.50
2	72.50%	90.63
3	75.00%	93.75
4	77.50%	96.88
5	80.00%	100.00
6	82.50%	103.13
7	85.00%	106.25
8	87.50%	109.38
9	90.00%	110.00
10	92.50%	113.14

Hyperbolic Profile is given by the equation,

$$\left(\frac{x^2}{a^2}\right) - \left(\frac{y^2}{b^2}\right) = 1 \ldots\ldots\ldots\ldots\ldots (3.1)$$

Where x is the radius at a point (or r), y is the height at a point, a is the throat radius (or $r_{th)\ nd}$ b is constant. The above equation can be written as,

$$\frac{r^2 + y^2}{r_{th}^2 b^2} = 1 \ \& \ b = \frac{r_{th}H_t}{\sqrt{r_t^2 r_{th}^2}} = \frac{r_{th}H_b}{\sqrt{r_b^2 r_{th}^2}} \ldots\ldots\ldots\ldots (3.2 \ \& \ 3.3)$$

As two hyperbolas are used in the model,

$$b_{top} = \frac{r_{th}H_t}{\sqrt{r_t^2 r_{th}^2}} \ \& \ b_{bottom} = \frac{r_{th}H_b}{\sqrt{r_b^2 r_{th}^2}} \ldots\ldots\ldots\ldots (3.4 \ \& \ 3.5)$$

Where x (or) r is the radius of point at a height y, a is throat radius, b is constant, $r_{th\ is}$ radius of throat, r_b is radius of base, r_t is radius of top and H_b is height of throat from shell bottom. Z is height from throat.

Radius at various levels are calculated using,

$$r_o = \sqrt{\left(1 + \frac{z^2}{b^2}\right) a^2} \ldots\ldots\ldots\ldots\ldots\ldots (3.6)$$

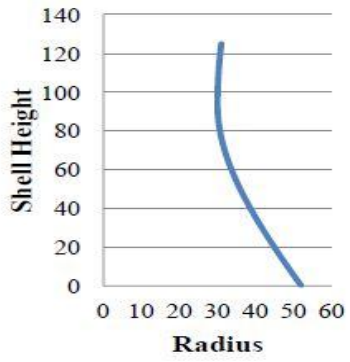

Figure 1.5. Radius - model with throat at 75%

Similarly, for all 8 models, radius at each level is calculated. For analysis, as per IS: 11504 – 1985 (clause 6.3.1 B-1.1) it must be possible to obtain information at 10° plan angle and not more than 5% of shell height. In this paper, the total number of elements are decided such that it is possible to obtain stress values to 2.5% of total height (i.e., 40 divisions along height) and 5° circumferentially (i.e., 72 plates in one level). STAAD.Pro is used for modeling and analysis.

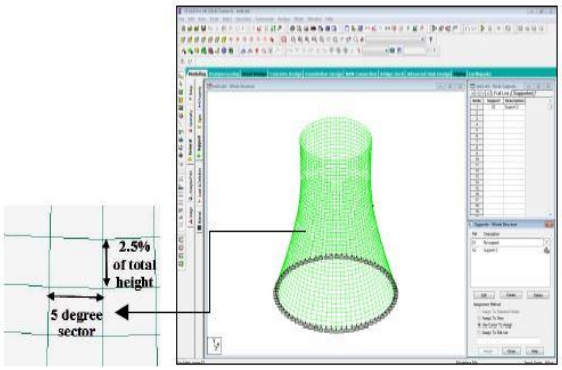

Figure 3.4. Degree of discretization in FE Model

Nodes

In every level there are 72 nodes. From level 0 to level 40, there are 41 levels. Therefore, in each model, Total number of nodes: 41 x 72 = 2952

Table 3.3 Node Numbers

angle	level 0	level 1	level ….	level 39	level 40
0^0	1	2	….	10	41
5^0	501	502	….	540	541
…	…	…	….	…	…
350^0	35001	35002	….	35040	35041
355^0	35501	35502	….	35540	35541

Plates

The shell structure is modeled using plate elements. In every level, there are 72 Plates. Therefore, in each model, Total number of plates: 40 x 72 = 2880.

Table 3.4 Plate Numbers

Segment	angle	Div 1	Div 2	….	Div 39	Div 40
1	$0^0 - 5^0$	101	201	….	3901	4001
2	$5^0 - 10^0$	101	202	….	3902	4002
…	…	…	…	….	…	…
71	$350^0 - 355^0$	171	271	….	3971	4071
72	$355^0 - 360^0$	172	272	….	3972	4072

Fig.3.4. Plates - NDCT model

Joint co-ordinates for all 2952 nodes are calculated and 2880 plate numbers are assigned with their respective node numbers. As specified by STAAD.Pro geometry modeling considerations, element aspect ratio is maintained within specific limits and while assigning nodes to an element in the input data, the nodes are specified either clockwise or counter clockwise. Uniform thickness of 300mm is chosen for all models and shell base is assumed fixed. M35 grade concrete is considered for analysis

Load calculation

Other than self-weight, the external applied loads that affect the cooling tower are dead loads, wind loads, effect of adjacent structures, imposed loads, foundation settlement loads, constructional loads, and thermal loads. The predominant forces acting on the cooling tower will result from wind or seismic loading. The reinforcement design of cooling tower is often controlled by the net difference between the tension due to wind load and compression due to dead load.

Wind force forms the major external applied loading in the design of cooling towers, and it also provides the most common means of determining the degree of lateral strength required by the towers. Wind load is calculated as pressure acting on each plate. Both vertical and circumferential variation if wind pressure is considered. The vertical variation if wind pressure is given by IS 875 – part 3 – 1987. And circumferential variation of wind pressure is given by IS 11504 – 1985.

Vertical Wind pressure distribution

IS 875 (Part 3) – 1987 determines wind pressures based on peak wind speed of 3 second gust with a return period of 50 years. The zones of basic wind seed at 10 m above ground at speeds of 33, 39, 44, 50 and 55 m/s are shown in the code on a wind map of the country. The design wind speed is calculated by considering the factors k1, k2, k3 related to probable life of structure, terrain, local topography and size of structure separately, and their combines effect is determined by multiplying the factors, the design wind pressure at any height above mean ground level shall be obtained by the following relationship between wind pressure and windvelocity:

$$\mathbf{P_Z = 0.6\, V_Z^{\,2}} \ldots\ldots\ldots\ldots (\mathbf{4.1})$$

Where

$\mathbf{P_Z}$ = design wind velocity in N/m^2 at height z, and

$\mathbf{V_Z}$ = design wind velocity in m/s at heightz.

Fig.4.1. Vertical distribution of wind pressure

Design Wind Speed (V_z) is The basic wind speed (V_b) for any site shall be modified to include the effects of risk level, terrain roughness, height and size of structure and local topography to get design wind velocity at any height (V_z) for the chosen structure.

$$\mathbf{V_Z = V_B\, K_1\, K_2\, K_3} \ldots\ldots\ldots\ldots (\mathbf{4.2})$$

V_z = design wind speed at any height *z* in m/s;

k_1 = probability factor (risk coefficient)

k_2 = terrain, height and structure size factor and

k_3 = topography factor

For analysis a basic wind speed of 50 m/s, terrain category I and structure class C is assumed. k2 is calculated at each level, k1 is taken as 1.08 and k3 as 1.0.

Using the above equations and values, wind pressure value for all 40 levels at the center of each shell along height is calculated.

Fig.4.2. Wind pressure variation in shell structure along height

Circumferential wind pressure distribution

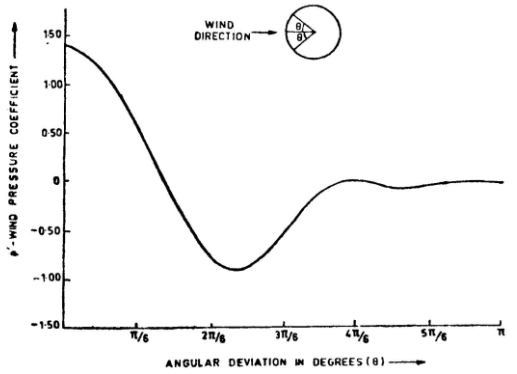

Figure 1.7. Circumferential wind pressure distribution

IS 11504 – 1987 gives the coefficient for circumferential variation of wind pressure in hyperbolic cooling towers. As per the code (clause 5.1.3 and 6.2 - A- 2), the wind pressure distribution on the outside of the shell is assumed to be symmetrical about the center line in the direction of wind.

For practical design these values may be increased by 10 percent to take into account geometrical imperfections. The wind pressure coefficient distribution around the shell is defined by the following graph

Circumferential Wind Pressure Coefficient Distribution

The distribution shall be used at all heights of the tower and includes an allowance for internal suction

$$p' \sum_{n=0}^{7} F_n \cos n\emptyset \ldots\ldots\ldots\ldots\ldots\ldots\ldots\ldots\ldots\ldots\ldots (4.3)$$

p' = design wind pressure coefficient,

F_n = Fourier coefficient of n^{th} term, and

θ = angular position measured from the incident wind direction in degrees.

Values of F_n for various values of n are tabulated below:

Table 4.1: Fourier Series F_n

N	F_n
0	-0.00071
1	+0.24611
2	+ 0.62296
3	+0.48833
4	+0.10756
5	- 0.09579
6	- 0.01142
7	+ 0.04551

With various values of F_n from the table, circumferential wind distribution coefficient for each 2.5° angle difference is calculated. Fig.4.4. shows the variation of the coefficient (p') in the structure's cross section. The coefficient is maximum at incident 0° and it slowly reduces below 0 and attains negative maximum (Suction) around 75°.

Circumferential variation of wind pressure

The actual design wind pressure on the shell is obtained by multiplying the basic wind pressure as given in IS: 875 by the coefficient p'. Hence individual values of pressure acting on all 2880 plates are calculated.

Dynamic effects of wind

As per IS 875 (Part 3) – 1987, Clause 7.1 Flexible slender structures and structural elements shall be investigated to ascertain the importance of wind induced oscillations or excitations along and across the direction of wind. In general, the following guidelines may be used for examining the problems of wind induced oscillations:

- Buildings and closed structures with a height to minimum lateral dimension ratio of more than about 5.0, or
- Buildings and structures whose natural frequency in the first mode is less than 1.0 Hz. (Natural frequency is (1/T), whereas the fundamental time period (T) may either be established by experimental observations on similar buildings or calculated by any rational method of analysis)

Any building or structure which satisfies either of the above two criteria shall be examined for dynamic effects of wind. If preliminary studies indicate that wind- induced oscillations are likely to be significant, investigations should be pursued with the aid of analytical methods or, if necessary, by means of wind tunnel tests on models.

Dynamic wind response

For calculation of along-wind load effects at a level s on a building/structure, the design hourly mean wind pressure at height z shall be multiplied by the Gust Factor. This factor is dependent on both the overall height h and the level s under consideration. A simplified Gust Factor method is given in the revised code IS 875 (Part 3) – 2015.

Note – 0<s<h s<z<h

Fig 4.5. Notations for heights

Gust factor is given by,

$$G = 1 + r\sqrt{\left[g_v^2 * B_s(1+\emptyset)^2 + \frac{H_s\, g_v^2\, S\, E}{\beta}\right]} \dots\dots\dots\dots\dots\dots (4.4)$$

r = roughness factor which is twice the longitudinal turbulence intensity $I_{h,i}$

g_v = peak factor for upwind velocity fluctuation, 3.0 for category 1 and 2 terrains and 4.0 for category 3 and 4 terrains.

Bs = background factor indicating the measure of slowly varying component of fluctuating wind load caused by the lower frequency wind speed variations =

$$\frac{1}{1+\frac{\sqrt{0.26(h-s)^2+0.46\, b_{sh}^2}}{L_h}}$$

b_{sh} = average breadth of the building/structure between heights s and h

L_h= measure of effective turbulence length scale at the height, h, in m

$= 85\left(\frac{h}{10}\right)^{0.25}$ for terrain category 1 to 3

$= 70\left(\frac{h}{10}\right)^{0.25}$ for terrain category 4

Φ= factor to account for the second order turbulence intensity

$= \frac{g_v * I_{h,i} * \sqrt{B_s}}{2}$

$I_{h,I}$= turbulence intensity at height h in terrain category i

H_s= height factor for the resonance response

$= 1+\left(\frac{s}{h}\right)^2$

S= size reduction factor given by:

$= \frac{1}{\left[1+\frac{3.5\, f_{ah}}{V_{h.d}}\right]\left[1+\frac{4\, f_a b_{oh}}{V_{h,d}}\right]}$

b_{oh}= average breadth of the building/structure between 0 and h.

E= spectrum of turbulence in the approaching wind stream

$= \frac{\pi N}{(1+70.8\, N^2)^{\frac{5}{6}}}$

N= effective reduced frequency

$= \frac{f_a L_h}{V_{h,d}}$

f_a= First mode natural frequency of the building/structure in along wind direction

$V_{h,d}$= design hourly mean wind speed at height, h in m/s

β= damping coefficient of the building/structure

g_R= peak factor for resonant response

$= \sqrt{[2\mathrm{In}(3600\, f_a)]}$

Calculation of Gust FactorAs per Eq. 4.4,

$$G = 1 + r\sqrt{\left[g_v^2 * B_s(1+\emptyset)^2 + \frac{H_s\, g_v^2\, S\, E}{\beta}\right]}$$

g_v = 3.0 for category I

Turbulence intensity Iz is given by clause 6.5, IS 875 (Part 3) – 2015

Terrain category 1

$$I_{z,1} = 03507 - 0.0535\, log_{10}\left(\frac{z}{z_{0,1}}\right)$$

Terrain category 2,

$$I_{z,2} = I_{z,1} + \frac{1}{7}(I_{z,4} - I_{z,1})$$

Terrain category 3

$$I_{z,3} = I_{z,1} + \frac{31}{7}(I_{z,4} - I_{z,1})$$

Terrain category 4

$$I_{z,1} = 0.466 - 0.1358\, log_{10}\left(\frac{z}{z_{0,1}}\right)$$

$z_{0,1}$ = 0.002 (for terrain category 1)

$I_{z,1}$ = 0.092

r =0.18466

As per Eq. 4.5

$$B_s = \frac{1}{1+\frac{\sqrt{0.26(h-s)^2+0.46\, b_{sh}^2}}{L_h}}$$

h =135 m

As per Eq. 4.6, $L_h = 85\left(\frac{h}{10}\right)^{0.25} = 162.93$

b_{sh} and Bs is calculated for each level and φ, H_s is calculated for each level using the formula given below

As per Eq. 4.8

Φ= $\frac{g_v * I_{h,i} * \sqrt{B_s}}{2}$

$H_s = 1+\left(\frac{s}{h}\right)^2$

f_a can be calculated using the formula,

$f_a = 1/T$, Where T is time period

$= \frac{1}{\frac{0.09\, H}{\sqrt{d}}}$

Here , f_a values have been obtained from STAAD Pro.

Table.4.2. First mode Natural frequency

Model Number	Throat Location in %	f_a
1	70%	1.117
2	72.5%	1.158
3	75%	1.197
4	77.5%	1.230
5	80%	1.252
6	82.5%	1.259
7	85%	1.249
8	87.5%	1.225

As per Eq. 4.13, $g_R = \sqrt{[2\mathrm{In}(3600\ \mathrm{f_a})]}$

As per Eq. 4.10,

$$S = \frac{1}{\left[1+\frac{3.5\,f_{ah}}{V_{h,d}}\right]\left[1+\frac{4\,f_a b_{oh}}{V_{h,d}}\right]}$$

As per Eq. 4.12 $N = \frac{f_a L_h}{V_{h,d}}$

As per Eq. 4.11 $E = \frac{\pi N}{(1+70.8\,N^2)^{\frac{5}{6}}}$

$\beta = 0.02$ (**For RCC**)

By calculating all the above parameters, Gust Factor G is calculation for each level .The value ranges from 1.54 to 162

Table.4.3. Gust Factor (Model 1)

Level	Gust Factor (G)	Level	Gust Factor (G)
1	1.545347	21	1.588617
2	1.547207	22	1.5909
3	1.549112	23	1.593162
4	1.55106	24	1.595398
5	1.55305	25	1.597605
6	1.55508	26	1.599775
7	1.557148	27	1.601906
8	1.559252	28	1.603992
9	1.561391	29	1.606031
10	1.56356	30	1.608021
11	1.565759	31	1.609961
12	1.567985	32	1.611853
13	1.570233	33	1.613694
14	1.572502	34	1.615481
15	1.574787	35	1.617212
16	1.577085	36	1.618885
17	1.579391	37	1.620498
18	1.581703	38	1.622051
19	1.584014	39	1.623542
20	1.58632	40	1.624973

Similarly for all models, Gust Factor at each level is calculated. To calculate the pressure (including gust effect) along height, Gust factor is multiplied with the pressure at each level. Here the pressure at each level is calculated with the modified k_2 factor ($_{@}$) (for hourly mean wind speed) as given by clause 6.4, IS 875 (Part 3) – 2015.

$$\mathbf{V_Z = V_B\, K_1\, K_2\, K_3\, K_4}$$

$$\boldsymbol{P_Z = 0.6\, V_z^2}$$

$$\boldsymbol{p_d = K_d\, K_a\, K_c\, p_z}$$

Here wind directionality factor kd, Area averaging factor ka, Combination factor Kc, cyclone factor k4 are taken as 1. The calculated Gust Factor is multiplied with pd to get the pressure at each level. The pressure on each plate is calculated by including the circumferential wind distribution. From the values, it is found that for the geometry considered here, only for the top 10 plates (25% of total height from top) pressure with gust factor is higher than the pressure calculated without considering dynamic response. Also this increase of pressure at the top is very close to the previous values. This is $\mathbf{K_2}$ because is mostly less than 1 for this geometry and thus it has reduced the pressure at each level. In this work, dynamic effects of wind are not considered in analysis as (i) the structure does not satisfy either of the criteria mentioned in section 4.4 and (ii) the design wind pressures with gust are slightly higher only in the top region, than static pressure.

Effect of adjacent structures

For taller and larger cooling towers the effect of adjacent structures in wind load plays a vital role, and hence it is important to derive the wind pressure distribution on the structure from wind tunnel experiments. Also for towers built at closer spacing, it is suggested to determine wind pressure distribution by model tests in a wind tunnel offering appropriate aerodynamic similitude. Such models shall include all adjacent topographical features, buildings and other structures which are likely to influence the wind load pattern on the tower significantly. This effect is not considered in this project.

Finite element analysis

The finite element method (FEM) is a numerical method for solving problems of engineering and mathematical physics. Finite element analysis (FEA) refers to procedure implementing the said method for solving complex engineering problems. The finite element method formulation results in a system of algebraic equations. The method yields approximate values of the unknowns at discrete number of points over the domain. In order to derive solution, a continuous domain is discretized into a set of discrete sub-domains, usually called finite elements. The simple equations that model these finite elements are then assembled into a larger system of equations that models the entire problem. FEM then uses variation methods from the calculus of variations to approximate a solution by minimizing an associated error function.

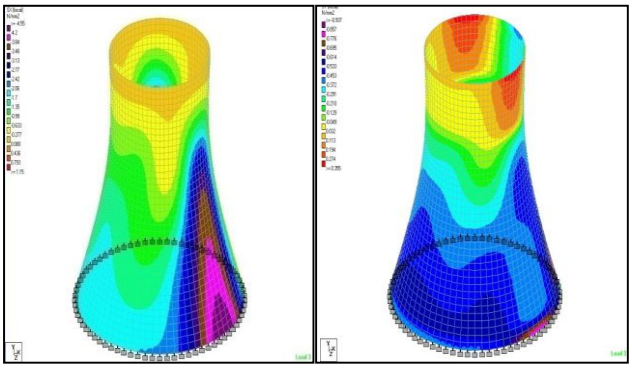

Figure 5.1. A typical Finite element mesh

In structural analysis, the most commonly used numerical approximation is the Finite Element Method. Here, FEM approximates a structure as an assembly of elements or components with various forms of connection between them and each element of which has an associated stiffness. Thus, a continuous system such as a plate or shell is modeled as a discrete system with a finite number of elements interconnected at finite number of nodes and the overall stiffness is the result of the addition of the stiffness of the various elements. The behaviour of individual elements is characterized by the element's stiffness (or flexibility) relation. The element stiffness matrices are assembled into a global stiffness matrix that represents the entire structure establishing system's stiffness or flexibility relation. To establish the stiffness (or flexibility) of a particular element, we can use the mechanics of materials approach for simple one-dimensional bar elements, and the elasticity approach for more complex two- and three-dimensional elements. The analytical and computational developments are best effected throughout by means of matrix algebra, solving partial differential equations.

Plate Element Analysis using STAAD Pro:

STAAD plate finite element is the simplest possible forms of plate/shell elements with only corner nodes and six degrees of freedom per node. As the plates used in the models have thickness less than one tenth of their span, they are termed as thin plates. In customary Kirchhoff- love theory for thin plates, strains normal to the plate mid surface are neglected. It is assumed that the plate thickness does not change after deformation and it is also assumed that there are no interactions in the normal direction between layers parallel to the middle surface. But in STAAD, plate analysis includes the transverse shear deformation in plate bending and thickness of plate is considered in out of plane shear calculation. Both Out of plane rotational stiffness and out of plane shear strain energy is usefully incorporated in the formulation of the plate bending component. As a result, the elements respond to Poisson boundary conditions which are considered to be more accurate than the customary Kirchhoff boundary conditions.

Analysis of cooling tower shell:

As discussed earlier in Chapter 3, the cooling tower shell is modeled with numerous finite plate elements. Fig.5.2 shows the membrane stresses and moments in a plate element.

SX and SY are membrane stresses represented as force/unit length/ unit thickness. Where SX is the membrane stress along the local X axis (meridional Stress) and SY is the membrane stress along the local Y axis (Hoop stress). The tower shell is considered to be fixed at the top of the columns in the finite element model. Analysis is done for self-weight, wind load and their combination. For all eight models, meridional stress (SX) and hoop stress (SY) values at the center of plates are obtained and their meridional and circumferential distributions are plotted and compared.

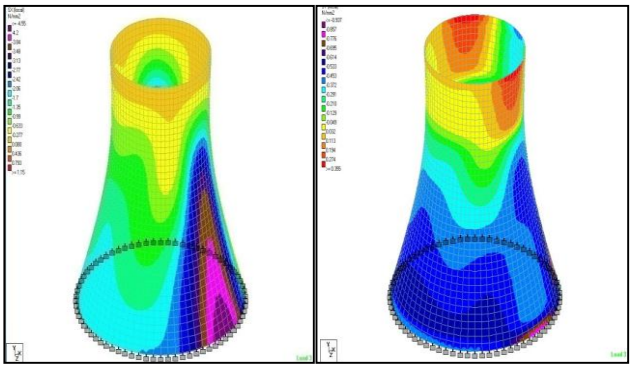

Figure 2.0 Stress contour for S.W+ W.L combination load case (a) SX (b) SY

RESULTS & DISCUSSION

For moderately sized towers, as per IS 11504 – 1985, clause 6.3.1, B-1.1, membrane analysis gives sufficiently satisfactory results. The analysis of tower shell should be carried out as per the elastic theory for thin shells either by classical methods or by numerical methods like finite differences or finite elements. Bending analysis is significant only for very large cooling towers.

This work discusses the effect of membrane stresses alone. Variation of meridional and hoop stresses for all 8 models along the height are plotted for self- weight, wind load and their combination.

Maximum wind pressure is on incident $\theta = 0°$ and maximum suction wind pressure is on $\theta = 75°$. Hence for wind load and S.W+W.L combination load cases graphs are plotted for plates at $\theta = 0°$ and $\theta = 75°$. Positive values denote tensile stress and negative values denote compressive stress on plates.

Variation of stresses due to Self-weight

The variation of self-weight along the height of cooling tower is plotted in fig.6.1 and fig.6.2. As self-weight at a level is uniform across the circumference, value is plotted only at $\theta = 0°$.

Self-weight induces compression. From fig.6.1, it is seen that, due to self-weight, distributions of meridional stress in all eight models are similar. However, from fig.6.2 it is seen that, their hoop stress distributions are different.

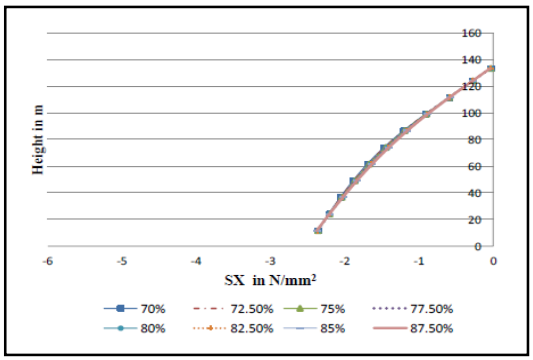

Figure 6.1. Meridional stress distribution due to self weight

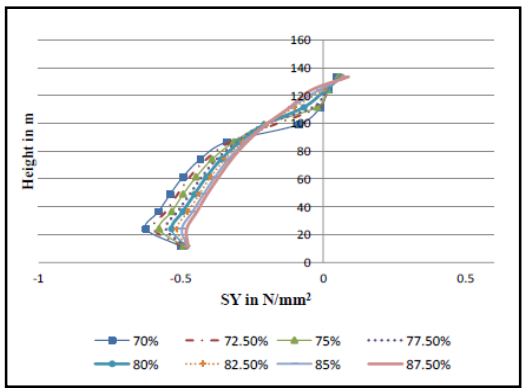

Figure 6.2. Hoop stress distribution to self weight

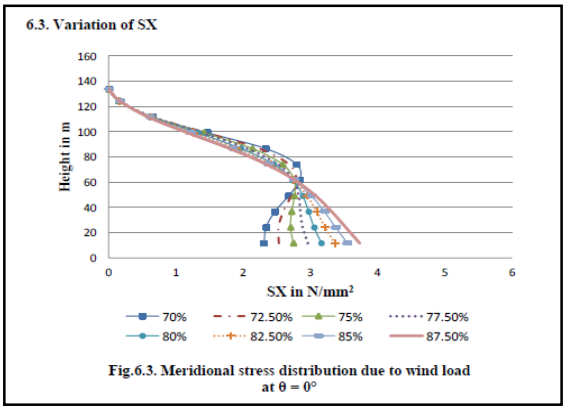

Figure 6.3. Meridional stress distribution due to wind load at θ = 0°

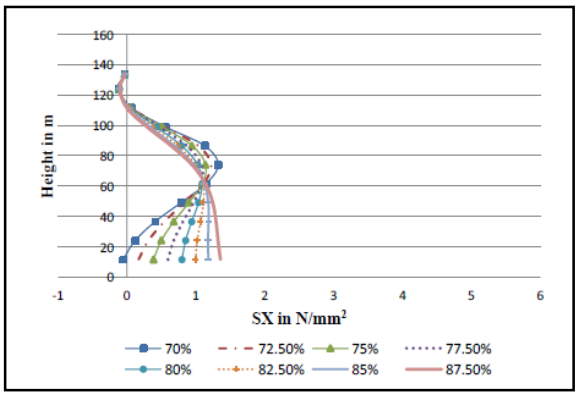

Figure 6.4. Meridional stress distribution due to S.W+W.L at θ = 0°

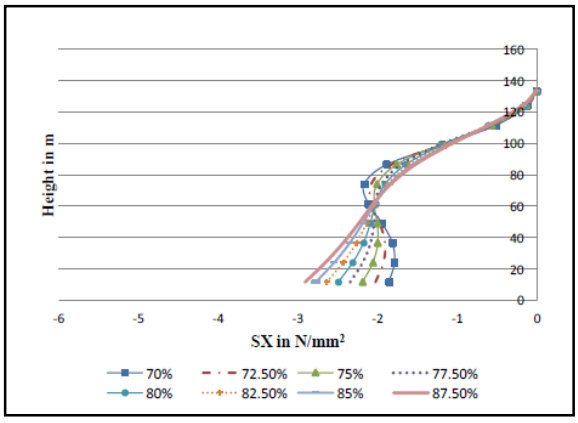

Figure 6.8. Meridional stress distribution due to wind load at θ = 75°

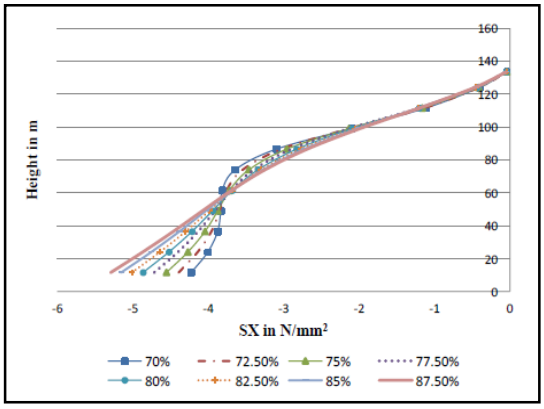

Figure 6.6. Hoop stress distribution due to S.W+W.L at θ = 75°

Variation of SX – Discussion

From fig.6.3 and fig.6.4 it is observed that at θ = 0°, self-weight reduces the net tension caused by wind load (fig.6.1). When throat is high, SX is maximum at bottom and decreases steadily as it approaches top. When throat is lowered SX increases from bottom up to a certain height which is approximately around mid- height of shell and thereafter it starts to decrease. The advantage of having lower throats is

mainly in the bottom portion of cooling tower. However due to the minimum reinforcement requirement this advantage may or may not be present when throat is very low.

As mentioned earlier for throat at 87.5% SX is less in top portion and is more at bottom where the overall reinforcement requirement is more due to the increased base diameter. Hence it is highly uneconomical to go for models with throat at higher location. The economical design with respect to SX would be to have a relatively lower throat and at the same time whose reinforcement requirement at bottom is close to minimum reinforcement requirement which will give additional benefit due to lower SX above shell mid height.

For θ = 75° (fig.6.5 & fig.6.6), compressive stresses due to self-weight increases the total compression induced by suction wind. Compressive stresses are more for higher throats. Hence models with lower throat are economical for concrete design as well.

Variation of SY

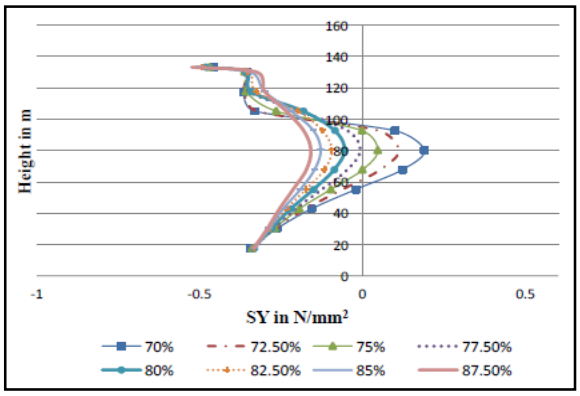

Figure 6.10. Hoop stress distribution due to wind load at θ = 0°

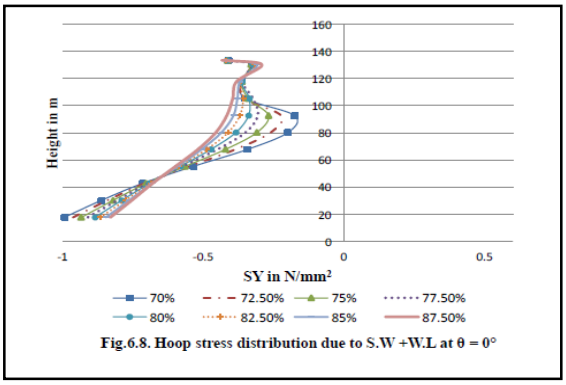

Figure 6.8. Hoop stress distribution due to S.W+W.L at θ = 0°

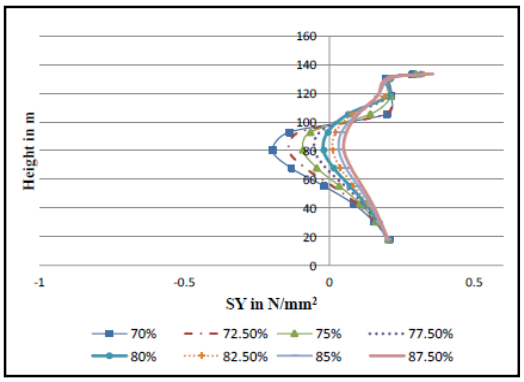

Figure 6.10. Hoop stress distribution due to wind load at θ = 75°

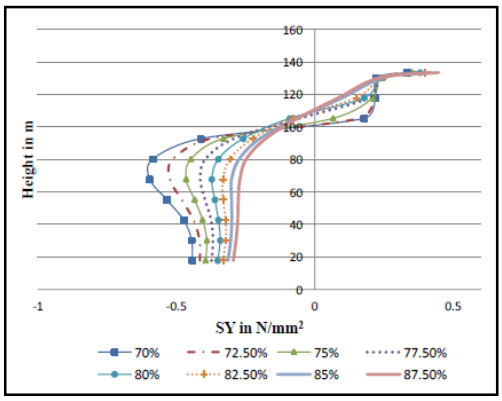

Figure 6.10. Hoop stress distribution due to S.W+W.L at θ = 75°

Variation of SY- discussion

In fig.6.7 it is observed that at θ = 0° hoop stresses induced by incident wind are tensile only in the middle portion (near the throat) of models with lower throats. Under the combined action of self-weight and wind, net hoop stresses are compressive for all 8 models (fig.6.8).

On incident face, at the bottom of the tower, SY (Compression) is low when throat is located at higher elevation. This behavior continues up to a certain height, and thereafter the trend gets reversed i.e., when throat is lowered SY also decreases, at a higher rate. Though SY for lower throat is maximum at the bottom, it decreases rapidly towards throat.

On suction side (θ = 75°), from fig.6.9 it is observed that, for models with lower throat, only middle portion of tower is subjected to compression. The compressive stresses due to self-weight increases the total compression induced by suction wind as seen from Fig.6.10. Hoop stresses are tensile above throat and compressive below throat. On suction side, both compressive and tensile hoop stresses are more for lower throats.

For most of the height, hoop stresses are compressive. When throat is high concrete design will be governed by stresses on incident face. As throat comes down, stresses on suction side

may govern concrete design. However, design of hoop reinforcement is based on stresses on suction side.

Variation of stresses along circumference

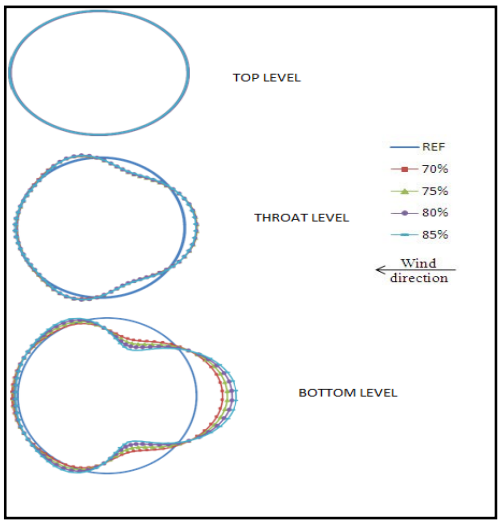

Figure 6.11. Variation of developed stress SX along the circumference of shell due to wind load.

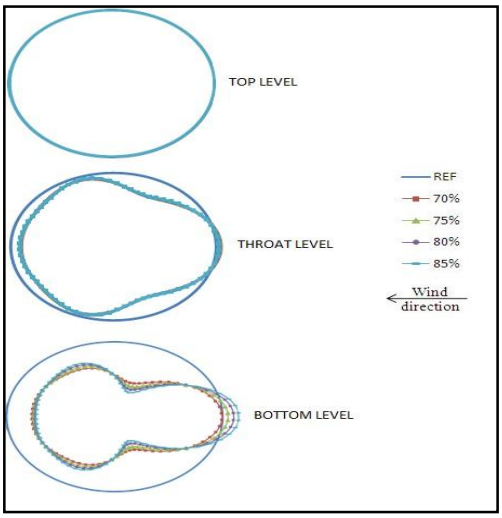

Figure 6.12. Variation of developed stress SX along the circumference of shell due to load combination (S.W+W.L)

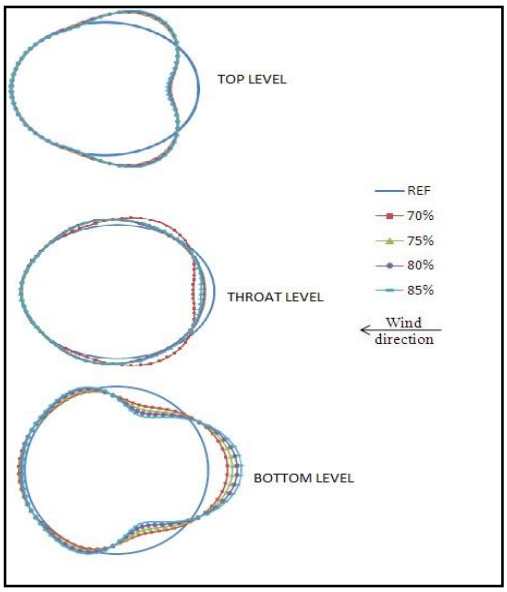

Figure 6.13. Variation of developedstress SY along the circumference of shell due to wind load

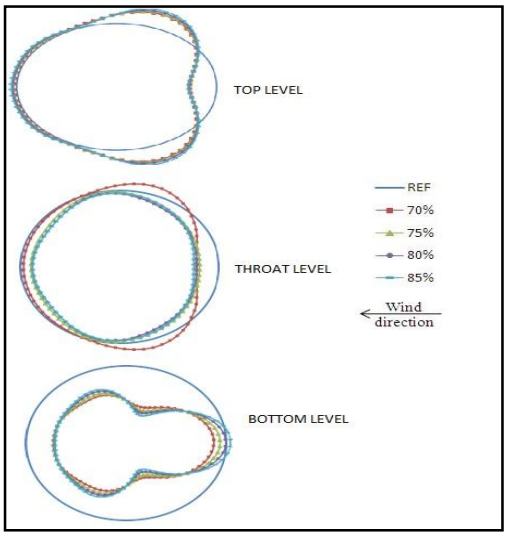

Figure 6.14. Variation of developed stress SY along the circumference of shell due to load combination (S.W+W.L)

Fig.6.11 and fig.6.12 showing circumferential variation of SX shows that tensile stresses due to wind load are reduced by the compressive stresses due to self- weight and net stresses are compressive in most of the region except incident face. The effect of throat variation is much in the bottom of the cooling tower and it gradually reduces to zero as we go to the top of cooling tower.

As per fig.6.13 and fig.6.14 circumferential variation of SY is similar to that of SX at the bottom. But the effect of throat variation is significant at throat than it is at bottom and top of cooling tower. At top level both incident face and suction face are subjected to higher hoop stresses. This implies the requirement of providing an upper ring beam.

CONCLUSION

- The base diameter, air intake opening height, tower height and throat diameter are determined by thermal considerations. Hence optimizing the location of throat is highly necessary in structural and economic considerations.
- Circumferential and meridional variation of both SX and SY shows that location of throat influences the stresses induced in cooling tower shell significantly.
- Variation of SX along height shows that the effect of throat variation is much in the bottom of the cooling tower and it gradually reduces to zero as we go to the top of cooling tower.
- Economical design with respect to SX would be to have a relatively lower throat and at the same time whose meridional reinforcement requirement at bottom is close to minimum reinforcement requirement. This gives additional benefit due to lower SX above shell mid-height.
- Hoop stresses are highly affected by changes in throat location mainly at throat level. Hoop stress variation is such that, higher throat location is not economical in incident face of cooling tower. Whereas very low throat location is not economical on the suction face.
- The effect of throat variation is significant at throat than it is at bottom and top of cooling tower. At top level both incident face and suction face are subjected to higher hoop stresses. This implies the significance of providing an upper ring beam.
- The range provided for throat location in the tower design considerations given by IS11504 can be used for towers of height less than 100m. For taller towers, optimization of throat location is required as it plays a vital part in the structural safety and economy.

REFERENCES

[1] Dieter Busch a, Reinhard Harte b, W. B. Kraetzig c, Ulrich Montag d 2002. New natural draft cooling tower of 200 m of height, Engineering Structures 24(2002), 1509–1521.

[2] Tejas G. Gaikwad, N. G. Gore, V. G. Sayagavi, Kiran Madhavi, Sandeep Pattiwar, 2014. Effect of Wind Loading on Analysis of Natural Draught Hyperbolic Cooling Tower, International Journal of Engineering and Advanced Technology,4(1), 34-39.

[3] Wilfried B. Kraetzig, 2009. From large natural draft cooling tower shells to chimneys of solar upwind power plants, International association for shell and spacial structures symposium, 28(09). 1-16

[4] IS 875 – 3 (1987): Code of practice for design loads for buildings and structures, Part – 3: Wind Loads.

[5] IS11504-1985 Criteria for structural design of reinforced concrete natural draught cooling towers

[6] BS-4485 Part - 4 (1986) Water cooling towers - Code of practice for structural design and construction.

[7] N. Prabhakar, 1990. Structural design aspects of Hyperbolic Towers, National seminar on cooling towers, 2(9) 65-72.

[8] Chiranjit mishra, a. ranjith, sanjith j, dr. b. m. kiran, 2015. Wind induced interference effects on natural draught cooling tower, International Journal of Progresses in Civil Engineering (IJPCE), 2(1), 6-12.

[9] G. Murali, C. M. Vivek Vardhan and B. V. Prasanth Kumar Reddy, 2012. Response of Cooling Towers to Wind Loads, APRN Journal of engineering and applied sciences,7(1), 114-120.

[10] Parth.R.Chhaya, Nizam.M.Mistry, Anuj.K.Chandiwala, 2014. A Review on Effect of Wind Loading on Natural Draught Hyperbolic Cooling Tower, International journal of advanced engineering and research development, 1(12), 47-50.

[11] Prashanth N, Sayeed Sulaiman, Aswath M U, 2013. To Study the effect of Seismic and Wind Loads on Hyperbolic Cooling Tower of Varying Dimension and RCC Shell Thickness, The international journal of science and technology. 1(3), 1-9.

[12] Priya Kulkarni, S.K. Kulkarni, 2015. Wind effect on Hyperbolic RCC Cooling Tower. International journal of current engineering and technology, 5(6), 3513-3517.

[13] Sachin Kulkarni, Prof. A.V. Kulkarni, 2014. Static and Dynamic Analysis of Hyperbolic Cooling Tower. Journal of civil engineering technology and research. 2(1), 39-61.

[14] Sithara T, Ance Mathew, 2016. Case study on the effect of static and dynamic loads on Hyperboloid Shell structure. 38(5), 233-237.

[15] X.X.Cheng, L. Zhao, Y.J. GE, 2013. Multiple Loading Effects on Wind Induced Static Performance of Super-Large Cooling Towers, International Journal of Structural Stability & Dynamics, 13(8), 1350039-1-1350039-21.